



## Scientific Background on the Nobel Prize in Physics 2021

“FOR GROUNDBREAKING CONTRIBUTIONS TO OUR  
UNDERSTANDING OF COMPLEX PHYSICAL SYSTEMS”

The Nobel Committee for Physics



## I. INTRODUCTION

This year’s Nobel Prize in Physics focuses upon the complexity of physical systems, from the largest scales experienced by humans, such as Earth’s climate, down to the microscopic structure and dynamics of mysterious and yet commonplace materials, such as glass. We recognize that scientists understand that no single prediction of anything can be taken as unassailable truth, and that without understanding the origins of variability we cannot understand the behavior of any system. Only then, for example, do we understand that global warming is real and attributable to humans. In the following we begin with a general background to provide a context for the discussion of specific contributions. A central emphasis is on the physical reality that the variability in the basic processes, from climate dynamics to frustrated materials, leads to the emergence of multiple length and time scales and hence is fundamental to interpretation of theory, experiment and observation.

### A. Instability and nonlinearity underlie multiscale complexity and stochasticity

The emergence of disorder from order, and with it multiple scales in space and time, is a characteristic of complex systems. Understanding the nature of that disorder presents an enormous scientific challenge. Natural questions include: Does it grow and space and time without bound? Does it choose a particular spatial structure or many spatial structures? Does that choice involve all of the degrees of freedom of a system or just a subset? Which subset?

The questions themselves have the same multi-scale structure as the phenomena they address.

A quintessential example is the transition of a laminar flow to a turbulent flow [e.g., 8, 66, 104], but in this and other nonlinear systems, characterizing the border between order and disorder is amongst the most challenging problems in physics. Indeed, advances in understanding multiscale physics have been prominent in turbulence theory and experiment [e.g., 10, 36, 64, 67, 88], and the linkages between statistical physics and hydrodynamic instability underlie the generality of the problem [92].

Turbulent thermal convection, such as what happens when we boil water, is an ideal setting for demonstrating the role of a myriad of scales in controlling macroscopic transport of heat and mass [23, 51]. This was on the mind of Edward Lorenz when he built his “toy model” of convection in the atmosphere [56], which is a Galerkin-modal truncation of the equations for Rayleigh-Bénard convection with stress-free boundary conditions on the

upper and lower boundaries [97]. The model is

$$\begin{aligned}\frac{dX}{dt} &= \sigma(Y - X), \\ \frac{dY}{dt} &= X(Ra - Z) - Y \quad \text{and} \\ \frac{dZ}{dt} &= XY - \beta Z,\end{aligned}$$

where  $X$  describes the intensity of convective motion,  $Y$  is the temperature difference between ascending and descending flow and  $Z$  is the deviation from linearity of the vertical temperature profile. The control parameters are the Prandtl Number,  $\sigma$ , which is a property of the fluid, the Rayleigh Number,  $Ra$ , which is the dimensionless buoyancy driving vertical fluid motions, and a constant factor  $\beta$ , characterizing the domain geometry.

The Lorenz system acts as a rich toy model of low-dimensional chaos. Since its origin the breadth and extension of studies has been so broad [e.g., 103] it would be difficult to enumerate them all. Key here are the facts that the solutions are bounded, (Fig. 1) and yet exhibit *sensitive dependence on initial conditions* (Fig. 2).

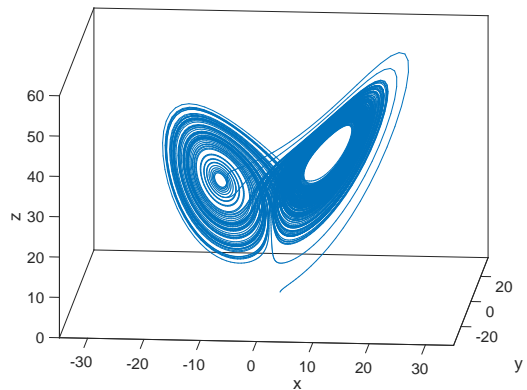


FIG. 1. Plot in  $(X, Y, Z)$  phase space of numerical simulation of a circuit version of Lorenz system at  $(\sigma, \beta, Ra) = (10, 8/3, 33.5)$ , from Weady *et al.* (2018).

Poincaré is generally credited with launching the field by discovering that the long-term behavior of the three-body problem was infinitely more complex than had been anticipated. In modern parlance he observed the tangling of *homoclinic orbits* (which are trajectories of a dynamical system flow joining a saddle equilibrium point to itself, residing at the intersection of the stable manifold and the unstable manifold of an equilibrium) and inferred the divergence of the perturbative solutions of the equations of motion. He recognized that the solar system could be viewed dynamically as a perturbation of the integrable Kepler (Hamiltonian) problem.

The complimentary pictures of statistical mechanics and hydrodynamics continue to inspire and challenge researchers. From the perspective of the phase space of a system, whereas in principle a complete description of the

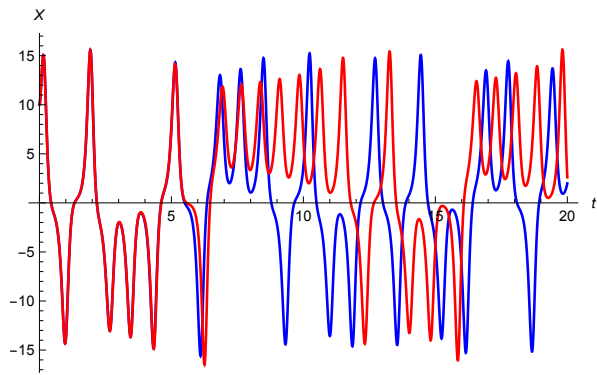


FIG. 2. Plot of  $X(t)$  of the Lorenz system with  $(\sigma, \beta, Ra) = (10, 8/3, 24.9)$  in which the initial data for all three variables are 10 (blue) or 10.01 (red). The divergence of the two solutions with slightly different initial conditions begins at  $t = 5.5$ ; this is sensitive dependence on initial conditions, often whimsically referred to as the “Butterfly Effect”.

evolution of the probability density of a system may be accessible via the Boltzmann, Fokker-Planck or Liouville equations [27], such high dimensional partial differential equations may be intransigent to useful analysis. In contrast, lower dimensional ordinary differential equations may exhibit shockingly complex chaotic dynamics [e.g., 35, 56, 103]. However, either formally [105] or in specific physical systems, such as those governing atmospheric dynamics [57], the effective dynamics may operate on a lower dimensional slow manifold. In consequence, it is reasonable to ask whether climate—the *signal*—is the slow manifold of weather—the *noise*. Of course, such a question is at the heart of the work being honored this year and is being asked across a vast range of disequilibrium systems where one replaces climate and weather with other systems. A central aspect of such questions is how one distinguishes between internal, external and emergent phenomena.

### B. Stochasticity and Disorder Imply Predictability

The relation between the signal and the noise in classical Brownian Motion assumes equipartition and hence thermal equilibrium. However, in systems out of equilibrium, the situation can be dramatically different. Giorgio Parisi [87] highlights the distinction between equilibrium and non-equilibrium systems as follows:

“But the situation is different for systems that are only slightly out of equilibrium. For example, imagine a system that cannot reach equilibrium because of high free-energy barriers (that may be of energetic or of entropic nature): this situation typically applies to disordered systems, such as spin glasses and structural glasses. Such a system will approach equilibrium slowly, by jumping from

one metastable state to another, and it could remain slightly out of equilibrium forever if continually perturbed with a slowly changing external field. In such systems we can expect a separation, by many orders of magnitude, between the microscopic time scale of the system (for example, that represented by the vibrations of individual atoms) and the macroscopic time needed to cross the barrier (for example, changes in the structure of the system itself). The system can then be considered to be essentially thermalized inside a metastable state, and so fluctuation-dissipation ideas can still be applied: the slowly changing overall state of the system is considered to be a small perturbation.”

This basic manner of thinking, be it for spin glasses or any other complex stochastic multiscale system, such as climate, characterize much of the landscape of the work being recognized this year. Indeed, it is essential to understand that noise and disorder influences all systems and can entirely determine the fate of some nonlinear dynamical systems. Thus, the concept of predictability is specious when one ignores the underlying causes of noise induced variability.

## II. CLIMATE PHYSICS: BACKGROUND AND HISTORY

Since Fourier’s studies of the Earth’s energy budget, shortwave solar radiation has been known as the central input of energy into the climate system. The spectral separation between this input, centered in the visible, and the output, in the infrared, underlies the nature of the habitability of any planet with an atmosphere that absorbs in the infrared. The heating effect of the absorption of solar radiation by  $\text{CO}_2$  and other gases was measured by Eunice Foote, but in 1861 John Tyndall [109] published a then technological *tour-de-force* of systematic absorption and emission of infrared radiation by a wide variety of gases, including water vapor and  $\text{CO}_2$ . This provided the experimental foundation for future studies of what we now call the “Greenhouse Effect”, and was a key ingredient in the major advance made in 1896 by Svante Arrhenius [6] (Nobel Laureate 1903), whose work we discuss more below. The absorption and emission of infrared radiation by Earth’s atmosphere is, apart from any other physics operative in physical climatology, a physically and computationally challenging area of broad relevance in planetary physics [91]. The history of physical climate science is described through major waypoints in the published literature collected by Archer & Pierrehumbert [4]. Indeed, the ease with which we can now all run online radiative transfer models, which we show next, might leave the likes of Tyndall shocked.

Figure 3 shows the results of the Moderate Resolution Atmospheric Transmission (MODTRAN) model, which

simulates the emission and absorption of infrared radiation in the Earth’s atmosphere. When  $\text{CO}_2$  is added to the atmosphere the infrared radiation escaping to space is reduced in the spectral range shown in the middle panel: A big “bite” appears at a wavenumber of about  $650\text{ cm}^{-1}$ , which is responsible for the reduction in outgoing radiative flux from the planet. Water vapor dominates the spectral range up to about  $500\text{ cm}^{-1}$  and then again at large wavenumber. The smaller “bite” centered at about  $1050\text{ cm}^{-1}$  is due to Ozone. In order to re-establish a steady state energy balance, the “wings” surrounding it, which are dominated by water vapor, must radiate at a higher temperature. In this example, the surface temperature increases by  $8.5\text{ }^\circ\text{C}$ . Water vapor dominates the spectral range up to about  $500\text{ cm}^{-1}$  and then again at large wavenumber. The smaller “bite” centered at about  $1050\text{ cm}^{-1}$  is due to Ozone.

Spectra such as seen in Figure 3 inform our understanding that the most potent Greenhouse Gas (GHG) in Earth’s atmosphere is water vapor, whose distribution we cannot directly control. It is simply not possible to “control” when, where and how much rain falls. Rather, atmospheric water vapor is controlled by the complex hydrological cycle and basic thermodynamics demonstrates that for every degree increase in temperature the atmosphere can hold approximately 7% more water. This is the basis of the so-called water vapor feedback. As the planet warms, the amount of water vapor in the atmosphere increases thereby increasing the temperature and so forth. Understanding *how* that water vapor is distributed through the action of the hydrologic cycle is a major challenge.

In principle we can control the Earth’s temperature by controlling other GHG concentrations. The simple question to ask is: Given an increase in atmospheric  $\text{CO}_2$  what are the consequences for global physical climatology? Like most clear questions in the physical sciences, the path towards an answer is a punctuated process, informed by both mistakes and successes. The “Keeling Curve” in Fig. 4 shows the key observations during our lifetimes. The curve is iconic both because of its analytical precision and its foreboding message; During the last eight glacial cycles—about 800,000 years—the  $\text{CO}_2$  concentration has not been higher than 300 ppm, with a maximum glacial-interglacial change of about 120 ppm and temperature anomalies greater than 10 K [25]. How does one model such a system that contains so many cogs and wheels?

### III. DEVELOPMENT OF MODEL HIERARCHIES

#### A. Energy balance models

The input of solar energy acts as the largest annual *external* periodic thermal forcing to the climate system. For this reason, we now know that any mathematical the-

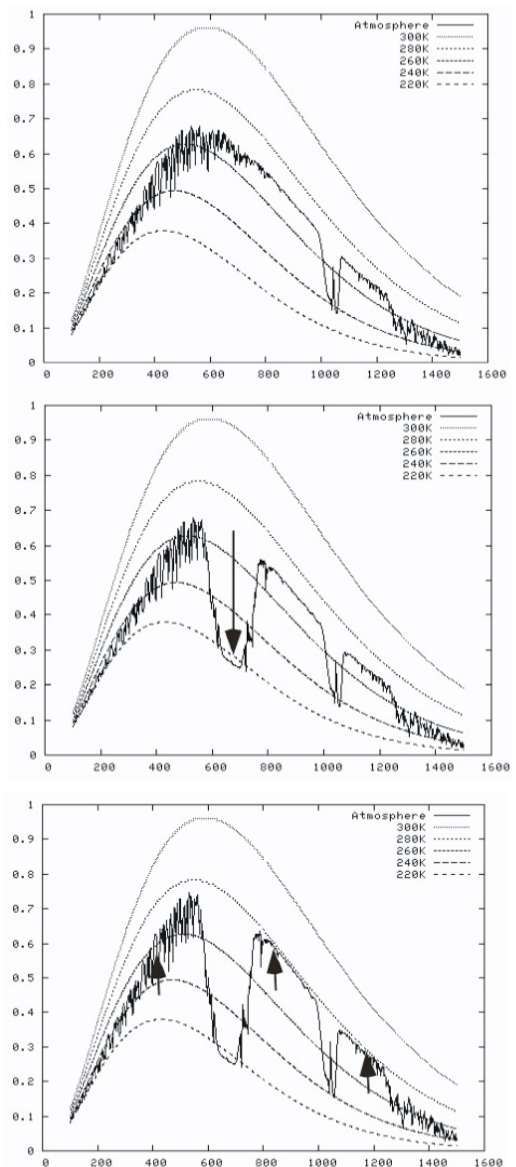


FIG. 3. The vertical axis is the total upward infrared energy flux in  $\text{Wm}^{-2}$  and the horizontal axis is wavenumber in  $\text{cm}^{-1}$ . The smooth curves are theoretical emission spectra of blackbodies at different temperatures. The jagged lines are spectra of infrared light at the top of the atmosphere looking down on Earth. The model demonstrates the effect of wavelength-selective greenhouse gases on Earth’s outgoing IR energy flux. Here we take an extreme version of increasing atmospheric  $\text{CO}_2$  from 0 ppm (top panel) to 1000 ppm (bottom two panels). In the top panel there is no  $\text{CO}_2$  in the atmosphere and the outgoing steady state flux is  $249\text{ Wm}^{-2}$ . In the middle panel, 1000 ppm  $\text{CO}_2$  is distributed through the atmosphere and the absorption “bite” (highlighted by the downward pointing black arrow) reduces the instantaneous flux escaping from the top of the atmosphere to  $223\text{ Wm}^{-2}$ . In the lowest panel, in order to re-establish steady state with  $249\text{ Wm}^{-2}$ , the “wings” surrounding it (dominated by water vapor and highlighted with the upward black arrows) must radiate at a higher temperature, in consequence of which the surface temperature increases by  $8.5\text{ }^\circ\text{C}$ . Online models are available at <http://climatemodels.uchicago.edu>.

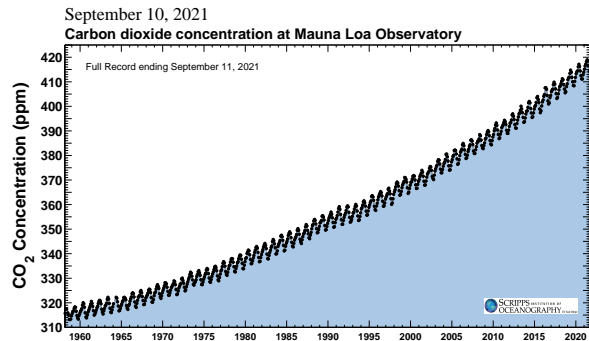


FIG. 4. The Keeling Curve, named after the late Charles Keeling who began the monitoring program. The curve shows monthly mean  $\text{CO}_2$  concentration from Mauna Loa, 1958-2021. (Data from Scripps Institution of Oceanography; <https://keelingcurve.ucsd.edu>.)

ory of climate must rely on the challenging edifice of explicitly time dependent differential equations to capture the time-evolution of climate subsystems on many time-scales. On the other hand numerical modeling, which marches forward the coupled equations of the entire system in the modality of weather forecasting, can incorporate time dependent forcing in a variety of ways. It is self-evident that the atmosphere, ocean, cryosphere, land masses and biosphere must obey the laws of thermodynamics. However, the myriad of time scales in the globally coupled system make determination of which subsystems are in what balance on a given time scale a challenging theoretical exercise.

The canonical class of energy balance models, now referred to as “Budyko-Sellers models” [15, 28, 78, 101], pits the incoming shortwave and outgoing longwave radiative fluxes against each other. In a mean annual, globally averaged sense we can write

$$C_P \frac{\partial T}{\partial t} = S_0(1 - \alpha) - \epsilon \sigma T^4, \quad (1)$$

where  $T$  is the temperature of the surface,  $C_P$  is its effective heat capacity,  $S_0$  and  $\alpha$  are the solar shortwave radiative flux and surface albedo respectively,  $\sigma$  is the Stefan-Boltzmann constant and  $\epsilon$  the emissivity. The fixed point for this simple model is

$$\epsilon \sigma T_{BP}^4 = S_0(1 - \alpha) \iff F_G^\uparrow = F_\odot^\downarrow, \quad (2)$$

or that the incoming solar flux ( $F_\odot^\downarrow$ ) is balanced by the upward surface flux ( $F_G^\uparrow$ ), which gives us the steady state temperature  $T_{BP} = \sqrt[4]{S_0(1 - \alpha)/\epsilon \sigma}$ . The atmosphere only enters into this result through the use of the planetary albedo  $\alpha$ , which is approximately 0.3 as determined from satellites, thereby including both highly reflective clouds (up to 0.9) and absorbing oceans (0.2). Hence,  $T_{BP}$  does not include the infrared contribution of the atmosphere and hence does not deal with

the greenhouse effect. In consequence, this is often referred to as a “bare planet” temperature and it is cold;  $T_{BP} \approx -15^\circ\text{C}$  [5, 91].

Now, the simplest means to see the infrared effects of the atmosphere is shown in Figure 5. In steady

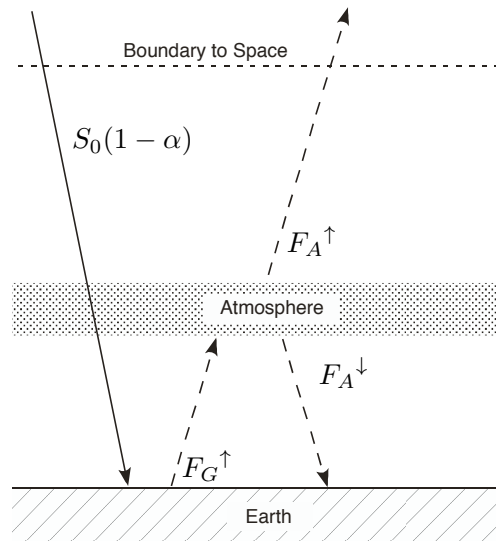


FIG. 5. Approximately as envisioned by Svante Arrhenius in 1896 [6], a “one-layer atmosphere” over Earth that absorbs and emits the outgoing infrared radiation from the surface  $F_G^\uparrow$ . We assume the outgoing atmospheric infrared emission is the same as the incoming, and that the atmosphere is isothermal, so that  $F_A^\downarrow = F_A^\uparrow \equiv F_A$ . Modified from [5].

state, balancing the fluxes in the atmospheric layer we have  $F_G = 2F_A$ , and using this at the surface we find  $F_\odot^\downarrow = F_A$  at the top of the atmosphere. The two key consequences are (a) the top of the atmosphere radiates to space at the (cold) bare planet temperature  $T_A = T_{BP}$ , and hence (b) the surface temperature is now a balmy  $T_G = 2^{1/4}T_{BP} \approx 34^\circ\text{C}$ .

Generalizing this to an  $N$ -layer atmosphere one finds that  $T_G = (1 + N)^{1/4}T_{BP}$  with the top of the atmosphere radiating to space at  $T_{BP}$ , with the clear implication of a runaway greenhouse effect that ignores the subtleties of the spectral absorption of greenhouse gases, feedbacks and many other effects. These leading order processes were understood by the polymath Svante Arrhenius. In 1896 [6], in a pioneering study of how absorption by  $\text{CO}_2$  would influence  $T_G$ , he built the scientific framework central to the atmospheric column models used in successively more complex treatments that have developed since then.

The effect now known as *band-saturation* was also understood by Arrhenius, who was using the then available state of the art spectroscopic data on  $\text{CO}_2$  and water vapor, and in particular that from the experiments of Tyndall [109]. In band-saturation the absorption increases linearly with temperature at low gas concentrations (or pressures) but with increasing concentration all infrared radiation entering a gas is absorbed. Not only did Arrhenius determine that the atmosphere is not sat-

urated, present spectroscopic measurements also show that  $\text{CO}_2$  is far from being saturated [91]. Moreover, we now understand that because of the vertical structure of both the gas concentration and the temperature, even were the atmosphere saturated,  $T_G$  can still rise because the radiation escapes to space from the thin diffuse upper layers that are not saturated. Finally, Knut Ångström argued that increasing  $\text{CO}_2$  would have little radiative impact because water vapor absorbs the infrared radiation that  $\text{CO}_2$  would absorb were its concentration to increase. Whereas this effect is operative in the lower-very high humidity-tropical atmosphere,  $\text{CO}_2$  influences the part of the infrared spectrum associated with the cold upper layers of the atmosphere radiating to space. In consequence, Ångström’s argument was superfluous [4, 91].

Arrhenius’ prediction, now referred to as “climate-sensitivity”, was to estimate the change in  $T_G$  upon a doubling of the atmospheric  $\text{CO}_2$ . Modern estimates have the range of 2.5-4°C and Arrhenius predicted approximately 6°C, which was limited by the accuracy of the absorption spectra and his treatment of the atmosphere roughly as shown in Figure 5. With the advent of modern spectra, this latter approximation underestimates the climate sensitivity because the effect described in the previous paragraph, wherein  $\text{CO}_2$  influences the range of the infrared spectrum associated with the cold upper layers of the atmosphere radiating to space cannot be incorporated. This underestimate was offset by the spectra he used.

Arrhenius also incorporated/highlighted other key components of modern physical climatology. In particular, the equator to pole energy imbalance, and the ice-albedo feedback. The latter effect, wherein a latitudinally dependent albedo in Eq. 1 underlies the two basic states of the climate system—cold and warm—is of central contemporary popular and technical interest with the rapidly evolving ice pack in the Arctic. Indeed, he made excellent predictions of the  $\text{CO}_2$  concentration during an ice age of 150 ppm, which we know from ice core research [25] was 180-200 ppm, as well as making estimates of how human coal consumption would lead to a doubling of atmospheric  $\text{CO}_2$ . All of this was done in a single paper in which he provided the conceptual scaffolding of contemporary atmospheric column models used in various incarnations today. In that sense, the central influences of anthropogenic greenhouse gas forcing on climate have been understood for a century and a quarter and Arrhenius’ work is truly prescient as a sheer intellectual *tour-de-force*, laying out the basic ingredients for analysis in the present day. See the discussion in [4].

## B. Generalized Deterministic Energy Balance Models (EBMs)

As introduced above in §III A, the simplest models treat global averages and focus principally on the ra-

diative transfer properties of the atmosphere. These are generalized to mean annual, zonally averaged (i.e., across latitudinal bands) quantities, whilst allowing for a latitudinal dependence of  $T_G$  and  $\alpha$  and meridional (longitudinal) heat transport. Such a framework admits a time-evolving planetary ice-line and hence a spatial ice-albedo feedback; if a perturbation slightly expands the ice cover, less energy is absorbed by the system, it cools further by Eq. 1, the ice expands further driving the cooling feedback. Indeed, such theories predict an abrupt transition to a completely ice-covered, or “snowball” Earth when the solar flux  $S_0$  is lowered by just a few percent. One such approach can be solved analytically [79] to find three fixed points; the snowball and the interglacial (present) states are both stable states, whereas that with approximately two-thirds ice cover is unstable. The approaches within this class of theories can be solved using spectral methods akin to those used in numerical simulations of the Navier-Stokes equations [77].

Although clear observational evidence of ice ages has long been known [2], the multiple global climate states predicted by a range of EBMs were results that were viewed as unrealistic theoretical predictions. However, contemporaneous interest in “nuclear winter,” wherein weapon suspended dust blocks incident solar radiation, constituted another interest in their predictions. Only in the last few decades has evidence been found for a global glaciation about 700 million years ago [54, 100] in the Neoproterozoic, highlighting the role of EBMs [15, 101] as quantitative tools.

Importantly, such theories capture the possible multiple states of the climate system and contain mathematically interesting and generalizable features that connect them to a broad class of multi-state systems appearing across many problems in physics, as described in §III D. In this sense, climate science stimulates research in other areas of physics.

## C. The Emergence of Numerical Climate Models

### 1. Prelude

All models are approximations to reality. All approximations, be they mathematical or the numerical implementation of formulae, break down in particular limits. The art in science is to make rational approximations. The rigor is associated with knowing with high precision the circumstances of the break down. Since the ready availability of large-scale computation, the term “model” in climate science nearly uniformly appears to be synonymous with Global Climate Models (GCMs) rather than EBMs. Contemporary GCMs operate in the same manner as did the original incarnations – by numerically solving the conservation of mass, momentum and energy throughout the atmosphere/ocean/ice system with parameterizations representing sub-grid scale physics (e.g., [38]). Some contemporary approaches to

improve GCMs use data assimilation [94] and test and implement high-resolution schemes [52]. Due to the complex nature of climate (particularly fluid) systems, GCMs are amongst the most sophisticated numerical models developed. Nonetheless, despite the enormous progress made in the development of GCMs, completely resolving the spatiotemporal processes in the climate system remains a challenge, particularly in the high latitudes [1]. Furthermore, because of the complex structure and high dimensional data produced by GCMs, it is not straightforward to extract the dominant physical processes on multiple time scales with the aim of interpreting their mutual interactions. Thus, GCMs operate like enormous coarse-grained weather forecasts; the global climate is represented by the output from a computational approximation of all of the known physics and, most importantly, parameterization of sub-grid-scale processes and often *ad-hoc* closure schemes connect different subsystems. Recent advances in climate models systematically embrace the concepts spearheaded by Klaus Hasselmann [42] that the chaotic dynamics in the weather underlie the variability on longer time scales and ultimately must be treated in models [e.g., 11, 20, 29, 59, 80, 81].

## 2. Origins

The difference between the incoming solar energy and the outgoing infrared energy is a function of latitude with a substantial excess of 5 PW between 40°N and 40°S. That energy is transported to the high latitudes by the motion of the atmosphere and the ocean and hence the quantitative fate and distribution of that heat focuses attention on the basic mechanisms of fluid flow and mixing in a rotating system. The atmosphere carries about 2/3 of the 5 PW and the remainder is transported by the ocean, but on different time scales and constrained by geography. Thus, the reality of theories and models is constrained by the treatment of these issues, as well as the cryosphere, due to the ice-albedo feedback.

During the 1950's large scale numerical weather forecasting originated at the Institute for Advanced Study in Princeton in a project led by Jule Charney and John von Neumann [19]. This naturally evolved roughly in parallel with the theoretical and experimental study of the detailed processes of atmospheric and oceanic dynamics generally referred to as *geophysical fluid dynamics-GFD* [114, 115]. Although over time a cultural difference between *GFD*, weather forecasting and climate modeling has lead to different communities they clearly share many similar goals if not approaches.

Many pioneers were recruited and/or visited for long stays and these people, including Bert Bolin, brought international expertise to the project [112]. Key here is the involvement of Joseph Smagorinsky, head of the U.S. Weather Bureau's General Circulation Research Laboratory, which later moved to Princeton to become the Geophysical Fluid Dynamics Laboratory, who recruited

Syukuro Manabe in 1959 and Kirk Bryan in 1961. The laboratory soon had a large staff of programmers.

Working independently, by 1960 Cecil E. Leith developed, coded and was running what could be considered as the first comprehensive atmosphere-only GCM (AGCM), the history is described in detail in a recent article [39]. The model had a domain up into the lower stratosphere and a representation of the hydrological cycle and clouds. Leith produced animations of the runs and hence also stood at the forefront of computer visualization.

## 3. Key Results

The numerical models being recognized [61–63] were built upon solid physics and can be considered as the first realizations of the dream of Arrhenius. Important earlier studies [60, 75] focused attention on how to incorporate known dynamical and radiative processes into a column model [62].

Manabe and Wetherald [62] treated the entire atmosphere as a single one-dimensional column with a given profile of relative humidity and greenhouse gas concentration. It evolves from an initial state (a) via radiative transfer, which is calculated given the spectra of greenhouse gases, the most important being water vapor, and (b) by *convective adjustment*. This process constitutes a parameterization of the vertical dynamics as follows. If a column evolves *solely* from radiative transfer, the lapse rate is  $\sim -15$  °C /km, far greater than observed. Now, the adiabatic lapse rate is  $\sim -10$  °C /km, but as air rises in a real atmosphere the condensation of water releases latent heat, which is largely responsible for the observed, or “moist”, lapse rate of  $\sim -6$  °C /km. To model this phenomena, whereby surface heating drives vertical motion, phase change and the concomitant release of heat, as soon as the temperature profile deviates from the moist lapse rate it is adjusted back to it. This is the *convective adjustment* scheme of Manabe and Strickler [61].

Manabe and Wetherald [62] noted that observations show rather little seasonal variation in the climatological latitudinal relative humidity profiles in the northern hemisphere, whereas the absolute humidity (saturation vapor pressure) will depend sensitively on temperature. Thus, Manabe and Wetherald [62] repeat the calculations of Manabe and Strickler [61] with the key difference between the two being that the later (earlier) paper used the given distribution of relative (absolute) humidity, which appropriately captures the “water vapor feedback” discussed above. As described in the arguments surrounding Figure 5, the upper layer of the atmosphere radiates to space at a low temperature and to get the energy balance there quantitatively correct, the relative humidity (embodying the most important greenhouse gas), the concentration of other greenhouse gases and the temperature must be captured. This confluence of effects led to the key result of Manabe and Wetherald [62], which is their calculation of climate sensitivity of 2.3 °C warming

per doubling of atmospheric CO<sub>2</sub> .

By 1975 Manabe and Wetherald [63] had substantially advanced their 1967 column treatment by solving the full equations for heat, mass, momentum and radiation around the globe—their first GCM—using a computer with about 0.5 MB of RAM. When they doubled CO<sub>2</sub> from 300 to 600 ppm the globally averaged surface temperature increased by 2.93 °C . The model assumes no transport of heat by the ocean, idealized topography and a fixed distribution of clouds amongst others.

As described in §III A, Arrhenius introduced the concept of climate sensitivity, which is still used today. However, one needs to distinguish the difference between the Arrhenius concept, or the *equilibrium climate sensitivity* (ECS), from the *transient climate sensitivity* (TCS). In ECS one envisions an instantaneous doubling of CO<sub>2</sub> and then calculates the new steady state energy balance with little veracity ascribed to the time it takes to reach that steady state. An extreme version of increasing atmospheric CO<sub>2</sub> from 0 ppm to 1000 ppm is shown in Figure 3, in which the Moderate Resolution Atmospheric Transmission (MODTRAN) model is used demonstrate the idea of the ECS. MODTRAN simulates the emission and absorption of infrared radiation in the atmosphere in the same manner as Manabe and Wetherald [62] but with modern spectral data and methods. When CO<sub>2</sub> is added to the atmosphere the infrared radiation escaping to space is reduced in the spectral range shown in the middle panel, but in order to re-establish a steady state, the “wings” surrounding it (dominated by water vapor) must radiate at a higher temperature, in consequence of which the surface temperature increases by 8.5 °C . This calculation rebalances the column energy in the same general sense as did Manabe and Wetherald [62, 63], and asks for the new surface temperature that achieves this.

Contemporary GCMs produce a climate sensitivity range of 2.5-4°C and the two rather different Manabe and Wetherald [62, 63] models produce a range 2.3-2.93°C . As described in §III A, we know why the Arrhenius result for ECS of approximately 6°C is an upper bound (accuracy of absorption spectra and an isothermal atmosphere) but the robustness of the Manabe and Wetherald [62, 63] results is remarkable, suggesting further that increasing model complexity may not increase fidelity of prediction. In reality the greenhouse gas profile is evolving over time, and hence so too is the response of the climate, which is what underlies TCS. Thus, humanity is really influenced by transient climate sensitivity. Both ECS and TCS are model dependent and it was Klaus Hasselmann who suggested a scheme for systematically assessing how models compare to evolving observations and what underlies variability in both.

## D. Stochastic Theories

Planetary climate reflects a myriad of interactions operating over a wide range of space and time scales. The spatially inhomogeneous distribution of shortwave radiative flux drives the atmosphere and ocean fluid-dynamically, leading to long-ranged communication through fluid advection and wave propagation [e.g., 31]. Whilst the GCMs described above attempt to capture these processes, computing a sufficient number of realizations to quantify variability is a perennial challenge. Therefore, a great deal of interest in how to quantify variability in a true statistical–central limit theorem–sense emerged in both observational and theoretical studies at the same time that the deterministic models of Manabe and his many collaborators were focusing on building GCMs.

To provide context, consider a global Budyko-Sellers EBM, such as shown in Eq. 1, and assume that the actual surface temperature  $T$  is not far from the average surface temperature  $T_S$ , such that  $T = T_S + x$  with  $|x| \ll |T_S|$  [e.g., 73]. The high-frequency fluctuations, such as those associated with weather, are represented as white noise,  $\eta(t)$ , with constant amplitude  $\bar{\sigma}$ , so that the time-evolution of  $x$  is represented by what is called an overdamped Ornstein-Uhlenbeck process, or generalized Langevin equation;

$$\frac{dx}{dt} = -\lambda x + \bar{\sigma}\eta(t), \quad (3)$$

with

$$\lambda = \frac{4\bar{\sigma}T_S^3 - S_0|\frac{\partial\alpha}{\partial T}|}{C_P}, \quad (4)$$

where  $\lambda$  represents the overall deterministic stability of the climate relative to the equilibrium temperature of  $T_S$ . The albedo sensitivity,  $\partial\alpha/\partial T$ , is negative, thereby exhibiting positive feedback, whereas the sensitivity of the outgoing longwave radiative flux is positive, thereby stabilizing deviations from  $T_S$ .

Analysis of observations of the spectral properties of pressure fields [76] in the context of signal processing motivated Mitchell [71] to posit an autonomous Langevin equation description of the ocean climate. At the same time Klaus Hasselmann was creatively using fundamental physics concepts to quantify the surface ocean wave spectra [40, 41], thereby building a deep appreciation for the nature of fluctuations on the sea-surface. Building on the intuition garnered from this research, basic concepts in turbulence and Lorenz’s chaotic weather (c.f., §I A), he derived a generalizable stochastic description of ocean climate in which the “noise” is associated with the “weather” as described above [42]. His work has provided both the motivation and the observational structure for climate scientists to address variability.

### 1. Outline of the Hasselmann [42] Stochastic Framework

Here we provide an interpretive and notationally uncluttered outline of the Hasselmann approach. Consider the climate system of interest to be described by a coupled set of governing equations represented by the vectors  $\mathbf{x} = (x_1, \dots, x_i)$  and  $\mathbf{y} = (y_1, \dots, y_j)$ , captured by two sets of functions  $f_i$  and  $g_j$  as

$$\dot{x}_i = f_i(x, y) \quad \text{and} \quad \dot{y}_j = g_j(x, y), \quad (5)$$

in which the characteristic time scales of evolution of all the  $x_i$  are much shorter than those of all of the  $y_i$ , where the latter treat the evolution of a “slowly” evolving large scale climate observables. With no loss of generality we further simplify the situation and treat  $x$  and  $y$  as scalar variables, allowing us to write the effective dynamics for  $y$  in terms of the fast variable as  $x = \langle x|y \rangle + x^*$ , where  $\langle x|y \rangle$  is the conditional average; the average of  $x$  conditioned on the state of  $y$ . Because  $x$  varies more rapidly than does  $y$ , we use the conditional dynamics in that for  $y$  as

$$\begin{aligned} g(x, y) \equiv g(\langle x|y \rangle + x^*, y) &\approx g(\langle x|y \rangle, y) + \partial_x g(\langle x|y \rangle, y) x^* \\ &\equiv -\frac{dU(y)}{dy} + \bar{\sigma}(y)\xi(t), \end{aligned}$$

where we have assumed that the rapid variations in the fast variable,  $x^*(t)$ , can be approximated as white noise with  $\langle \xi(t)\xi(t') \rangle = \delta(t-t')$ , an amplitude that depends on the state of the slow variable,  $\sigma(y)$ , and the deterministic dynamics that is interpreted as a drift force of the potential  $U(y)$ . Finally, when the intensity of the noise is small, the system will spend a long period of time near a fixed point, say  $y_E$ , around which the drift force can be expanded and the noise amplitude is ostensibly constant. Then the dynamics of the climate variable  $y(t)$  is reduced to an Ornstein-Uhlenbeck process of the form of Eq. 3, viz.,

$$\frac{dy}{dt} = -\Lambda y + \bar{\sigma}\xi(t). \quad (6)$$

This treatment in terms of Brownian motion concepts allows for the study of climate variables in the framework of stochastic differential equations. For example, in addition to studying the state of the system via Eq. 6, one can study the probability of the system being in a given state at a given time, because to every Langevin equation there exists a Fokker-Planck equation [e.g., 22]: This is a framework particularly useful in interpretation of climatological observations. Moreover, the solution to Eq. 6 gives the auto-correlation function,  $R(\tau) = \langle y(t)y(t+\tau) \rangle$ , the Fourier transform of which is the power spectrum,

$$P(\omega) = \bar{\sigma}^2 / (\Lambda^2 + \omega^2),$$

showing (a) the red noise response of the white noise process in Eq. 6 and (b) the most basic form of the fluctuation-dissipation theorem, tying the noise intensity

to that of the variance of the process itself, viz.,  $\langle y^2 \rangle = \bar{\sigma}^2 / (2\Lambda)$ .

It is important to emphasize that, unlike Mitchell, Hasselmann did not invoke Eq.(6) directly as an observationally motivated ansatz. Rather, he begins with Eqs.(5), which are better suited as a framework for stochastic parameterizations in climate models [e.g., 11, 20, 29, 59, 80, 81]. Importantly, there are of course an enormous range of time scales in the dynamical system that is climate and the existence of clear separations are at the heart of modern understanding of climate variability [e.g., 29]. Central to Hasselmann’s approach is the deterministic averaging described above, giving a coupled slow-fast deterministic system controlled by a multiplicative noise correction to the averaged forcing. As described by Culina *et al.* [20], this aspect has only recently been rigorously justified, but under more restrictive conditions than proposed by Hasselmann.

As shown in Fig. 6, while the spectrum grows as the frequency decreases, we expect eventual saturation because of the finite dissipation  $\Lambda$ . However, it has been shown by Hasselmann, Wunsch [e.g., see 113, and refs therein] and others that the ocean has an impressively long memory of events that can be hundreds to thousands of years old. Moreover, on the decadal time scales of relevance to humans, evidence is consistent with the memory being effectively infinite. Hence, this suggests a potential self-similarity or fractal character, in which multiple time scales provide different classes (e.g., brown, white, red, pink) of stochastic processes [72]. Therefore, the basic observation that a data record can be nonstationary, have a growing variance and a difficult to measure mean, are amongst the basic tenets of climate variability emerging from Hasselmann’s work on the analogy with Brownian motion.

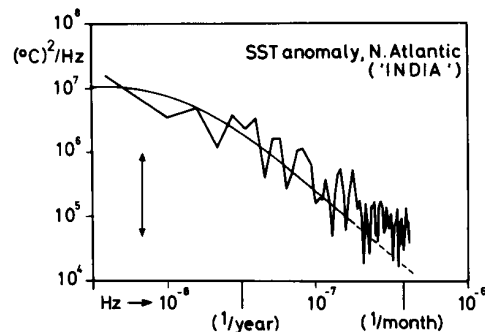


FIG. 6. The first application of the Hasselmann stochastic model [42] for climate variability to climate data [26]. The spectrum of the Sea Surface Temperature (SST) in the period 1949-1964 in the North Atlantic. The 95% confidence interval is given by the double headed arrow and  $\Lambda^{-1} = 4.5$  months.

Clearly this approach can, and has been, generalized and taken into many directions in this and many other fields. However, the theoretical framework in which one might fruitfully treat climate data, and hence climate predictability and variability, as a stochastic process is

traced to Mitchell [71] and Hasselmann [42] the latter of whom convincingly applied it to data with Frankignoul, as seen in Fig. 6. As is the case with most good ideas, they have as many approximations and limitations as they have new approaches and ideas that are born from them. In particular, as noted above, identifying a distinct spectral gap in observations, which would justify the assumption of time scale separation, depends on the data used. Nonetheless, because of Hasselmann’s theory, the typical null hypothesis for climate variability is a red power spectrum [65, 113].

#### IV. USING OBSERVATIONS TO TEST MODELS

From the perspective of laboratory science, using experimental measurements to test theory is such a self-evident step in the scientific method that it goes without saying. However physical cosmology and physical climatology are *observational sciences* – practitioners observe that which nature allows.

Decades before the satellite era, understanding atmospheric and oceanic dynamics relied on sparse observations. For example, much of the theoretical and observational focus before the International Geophysical Year (1957-58), when large scale systematic observational programs were launched, was centered around regions, such as the poles [58, 110], or the behavior of currents, such as the Gulf Stream, and the general oceanic and atmospheric circulation, motivated by the theories of Jacob Bjerknes, George Carrier, Walter Munk, Carl Rossby and Henry Stommel. These problems pushed the boundaries of mathematical and numerical modeling. Indeed, partly in consequence of the lack of observational data, that the numerical forecasting group at the Institute for Advanced Study discussed in §III C was formed.

As the 1922 Nobel Laureate Niels Bohr is famously quoted as saying, “Prediction is very difficult, especially if it’s about the future!”. Our principal tools for understanding the future of climate are the GCMs pioneered by Syukuro Manabe and his colleagues. One predicts, or “projects” in the parlance of the field, and waits to see what happens. Certainly, the future will always await our arrival, but the idea of Klaus Hasselmann was to use models *and* observations to ask what circumstances lead the climate to its present state? Natural variability or the increase in GHG concentrations due to human activity?

##### A. Fingerprinting

In order to assess whether climate models are faithfully reproducing the signal from the natural variability, Hasselmann’s interest in stochastic climate dynamics lead naturally to his creation of a framework to systematically compare climate models and observations. This was accomplished in three papers from 1979–1997 [43–45].

In his first paper in this series [43] Hasselmann notes that despite the conceptual analogies with data from single gridpoints, it is a challenge to deal with the vector field structure of the climate signal. Namely, in reference to the approach from single gridpoints, “...the question whether or not the response pattern, as a whole or in part, is statistically significant, *clearly cannot be resolved by such an approach.*”, and his work provides the framework from purely spatial data [43] to spatio-temporal data [44, 45]. Importantly, he shows how optimal detection techniques reveal understanding of the nature of the natural variability in the climate system or the “noise”. Namely, detection of a signal may not necessarily be associated with parts of the data where that signal is strongest, but rather where the noise is the weakest, thereby revealing a more nuanced physical interpretation of components of the system.

Fingerprinting methods identify climate change based on the physics governing the system through the use of climate model runs. The so-called “optimal fingerprinting” method is a *spatio-temporal* generalization of multivariate regression adapted to the detection of climate change and the attribution of change to externally forced climate signals [48]. Spatio-temporal fingerprints, such as the time varying three-dimensional changes in GHG concentrations, provide a means of discrimination between observed changes and natural variability. Through the years of refinement [45–49], the procedure is far more rigorous, nuanced and comprehensive than is comparison of model simulations with observations alone.

One begins with a filtered version of the observed record, given by the vector  $\mathbf{y}$ , and the regression takes a standard form  $\mathbf{y} = \mathbf{X}\mathbf{a} + \mathbf{u}$  where the matrix  $\mathbf{X}$  contains the estimated response patterns to the external forcings, or signals, that are of interest,  $\mathbf{a}$  is a vector of scaling factors that adjusts the amplitudes of those patterns and  $\mathbf{u}$  represents internal climate variability, typically assumed to be a Gaussian random vector with covariance matrix  $\mathbf{C}$ . The vector  $\mathbf{a}$  is estimated in terms of  $\mathbf{C}$ ,  $\mathbf{X}$  and  $\mathbf{y}$  with a variety of statistical techniques, where  $\mathbf{X}$  contains signals estimated with one or another models, either a GCM or EBM, to create “internal variability” with a complex spatio-temporal structure. For an observed response to be attributed to anthropogenic forcing,  $\mathbf{X}$  must contain separate natural and anthropogenic responses and hence  $\mathbf{a}$  must account for possible errors in forcing amplitude tuned to match the model to the observations. In this manner, detection and attribution are determined through a combination of physical reasoning and evaluation of specific hypotheses concerning the scaling factors within in  $\mathbf{a}$ . Importantly, the results rely on estimation of the exact fingerprint amplitudes from *observations*, and are independent of whether or not the climate models used correctly simulate the fingerprint amplitudes [e.g., 48, 49].

In a recent article, “Celebrating the anniversary of three key events in climate change science”, Santer and colleagues [98] reflect upon the progress during the four

decades since the 1979 “Charney Report” [19], which was the same year as Hasselmann’s first paper on how models and observations can be self-consistently compared [43]. There are four sections to the paper [98], the first being a summary of the Charney Report and the second titled “Hasselmann’s optimal detection paper” [43], which the authors refer to as ‘the first serious effort to provide a sound statistical framework for identifying a human-caused warming signal.’. This approach was a departure from previous work in univariate statistics:

Instead of looking for a needle in a tiny corner of a large haystack (and then proceeding to search the next tiny corner), Hasselmann advocated for a more efficient strategy - searching the entire haystack simultaneously...He also pointed out that theory, observations and models provide considerable information about signal and noise properties...These unique signal characteristics (or ‘fingerprints’) can be used to distinguish climate signals from climate noise.

From the Charney report, which relied on basic theory and early climate model simulations, there was clear recognition that fossil fuel burning would yield an appreciable global warming signal [19]. Klaus Hasselmann’s paper [43] outlined a rational approach for detecting this signal. Satellite-borne microwave sounders began to monitor atmospheric temperature, providing global patterns of multi-decadal climate change and natural internal variability information required for successful application of Hasselmann’s signal detection method.

Hasselmann’s paper was a statistical roadmap for hundreds of subsequent climate change detection and attribution (D&A) studies...[and]...provided strong scientific support for the conclusion reached by the IPCC in 2013: “It is extremely likely that human influence has been the dominant cause of the observed warming since the mid-20th century”

## V. THE VASTNESS OF THE LANDSCAPE OF DISORDER

### A. Replicas, Spin Glasses and Frustration.

The term “spin glass” was coined in the early 1970’s to describe disordered magnetic systems that appeared to have a phase transition to a state in which each magnetic atom was stably aligned, but with the essential proviso that the alignment direction varies randomly between atoms. Imagine a triangle with magnets placed on the three corners. The magnets can have either their

north poles up or down. Under intuitive circumstances, say upon placing the triangle in an external field pointing up or down perpendicular to its plane, one might imagine all three *either* up *or* down. Now we impose an “antiferromagnetic” constraint that any adjacent pair must have the opposite orientation. When two magnets satisfy the constraint, two others do not and no amount of flipping orientations will satisfy the constraint – the system is “frustrated”. This extremely idealized setting is one of the simplest means to see how spin glasses and other systems are frustrated.

Many frustrated systems are frustrated in their own ways and there are *many* from which to choose, including “structural” or “ordinary” glasses and “marginal” or “Gardner” glasses. This is not the forum to discuss the vast range of glassy systems, but a common feature in such systems is that when they are rapidly quenched they are unable to access equilibrium, and persist in occupying a plethora of very long-lived metastable states. Whence, a given experimental system typically has a unique measurement, numerical and/or conceptual protocol. That system specificity has remained a central challenge in the field from its inception [e.g., 12, 68, 96]. Philip Anderson (Nobel Laureate 1977) argued that “The history of spin glass may be the best example I know of the dictum that a real scientific mystery is worth pursuing to the ends of the Earth for its own sake, independently of any obvious practical importance or intellectual glamour.” [3].

### B. Solving the Replica Symmetry Breaking Problem

For brevity of illustration we can consider a spin glass as system of impurities or spins with a Hamiltonian

$$H = - \sum_{i,k} J_{ik} \sigma_i \sigma_k, \quad (7)$$

where the  $J_{ik}$  are uncorrelated Gaussian random variables with zero mean and variance  $\overline{J_{ik}^2} = K_{ik}$ . Frustration emerges by allowing both ferromagnetic and anti-ferromagnetic couplings, and hence we expect a “corrugated” energy landscape with many long-lived metastable states. Within this framework, we can sketch the developments in general heuristic terms. Edwards and Anderson [24] considered a short-ranged interaction so that  $K_{ik}$  decreases rapidly with  $i - k$  distance. Importantly, they constructed an order parameter for the spin glass phase that is the projection of a spin onto its original orientation, allowing one to neglect long range spatial ordering and instead consider long range temporal ordering. Thus, upon waiting for a long period of time, if their order parameter is finite the spins “remember” their original orientation and in that sense form a glass. Moreover, in order to average over macroscopic samples wherein a vast number of different configurations of the  $J_{ik}$  are operative, they introduced the so-called “replica

trick” making  $n$  copies or replicas of the partition function viz.,

$$\ln Z = \lim_{n \rightarrow 0} \frac{Z^n - 1}{n}, \quad (8)$$

thereby allowing properly averaged thermodynamic calculations,  $F = -kT \langle \ln Z \rangle_{\text{ave}}$ .

In the same year Sherrington and Kirkpatrick [102] came up with an infinite dimensional version of the Edwards and Anderson model, so that  $K_{ik} = N^{-1}$ , where  $N$  denotes the total number of spins. Whilst this allowed for a valid mean-field calculation, it also revealed a paradox; the entropy became negative at low temperature. Due to the many states with very nearly equal energies and no clear symmetry, computing convergent solutions was a great challenge. The challenge, however, led to the idea of simulated annealing [53]. In quick succession Thouless (Nobel Laureate 2016), Anderson and Palmer [106] resolved the negative entropy problem, but were left with the question of the stability of their solutions, and then de Almeida and Thouless [21] pointed the finger at the problem that “replica symmetry” was assumed. This led to calculations of broken replica symmetry by Blandin [13], and by Bray and Moore [14], but the subtleties of just how to break replica symmetry were still illusive.

Giorgio Parisi solved the problem of replica symmetry breaking by realizing that, in contrast to ferromagnets which have only two “pure states” (up/down) in the ordered phase, there must be an infinite number within the ordered phase of the spin glass [82, 83]. Not only did this provide the solution, but it had a stunning array of extensions to a wide range of spin-glass and other systems [68, 69, 84–86].

In order to realize the infinitude of states, Parisi’s great leap was to introduce a new order parameter;

$$q_{\alpha\beta} = \frac{1}{N} \sum_i \langle \sigma_i \rangle_\alpha \langle \sigma_i \rangle_\beta, \quad (9)$$

wherein  $\alpha$  and  $\beta$  are replicas. All of the  $q_{\alpha\alpha}$  are equivalent, representing the average overlaps of the states within a given replica, and the off-diagonal terms measure the degree to which  $\alpha$  and  $\beta$  resemble each other. Namely, they describe the average overlap between states belonging to replica solution  $\alpha$  and those belonging to replica solution  $\beta$ . In the glassy phase there is no unique locally stable thermodynamic state, but *many* states, each replica of which corresponds to a different solution to the mean-field equations. These solutions are clusters of states in the  $N$ -dimensional configuration space of the  $N$  spins. The mathematics are beyond the scope of this venue. A key concept it called *ultrametricity*, which is a functional version of the triangle inequality, which we all know from early school days; the sum of the lengths of any two sides of a triangle are greater than or equal to the length of the third. Here, ultrametricity can be characterized using a network describing the states of the system and one finds that upon choosing any three

states at random, at least two overlaps are equal so that the disorder-average distribution of overlaps is

$$P(q) = \sum_{\alpha,\beta} w_\alpha w_\beta \delta(q - q_{\alpha\beta}), \quad (10)$$

where the  $w$ ’s are Boltzmann weights.

### C. Applications and Implications

The broad reach of broken replica symmetry concepts and methods has exploded since Parisi’s original work. In particular, Parisi and his collaborators have shown that in John Hopfield’s neural network model [50], and its many offspring, the multiple memories stored in the network correspond to the multiple equilibria of the spin glass. Moreover, their methods allowed them to address the classical optimization problem of the traveling salesman who stops at many local minima but of course the global minimum/minima are the targets of interest [68]. At the time at which the book was published, David Thouless wrote [107]:

I feel that the spin glass experts are like settlers encamped in hostile territory. They have interesting observations to make, but have not learned how to communicate with the earlier settlers. In some of the papers on neural nets there is barely a reference to work by scientists outside the spin glass community.

Clearly in the more than three decades since, the early settlers have colonized widely across many communities. These include (a) providing a basic understanding of why some optimization tasks are easy and why some are very difficult (see [70] and Refs therein), (b) the random first order theory of structural glasses and (c) the geometric theory of jamming in hard spheres, which is an extremely successful application of mean-field broken replica symmetry, applying as it does from two- to infinite-dimensions [89]. The approach sets the agenda for experiments in classical granular matter [9] and is confirmed in detailed numerical analyses [16, 17, 95] in equilibrium and under slow compression [93]. Moreover, the marginal phase predicted by the replica theory of glasses, has been directly observed experimentally in a slowly densifying colloidal glass [37]. Importantly, experimental evidence of replica symmetry breaking has been provided in systems using random lasers [30, 33, 99, 108], in plane cavity lasers without disorder but with frustration between interacting lasing modes without added disorder [7, 74], and in nonlinear optical propagation through photorefractive disordered waveguides [90]. Finally, the nature of the random laser system allows for the concomitant observation of replica symmetry breaking and connection between spin-glasses and turbulence [34], particularly nonlinear wave interactions, which link the early work of Hasselmann [40, 41] to that of Parisi and to the

role of disorder and fluctuations in complex systems in general.

### Random Lasers and Replica Symmetry Breaking

As noted above, one of the exciting areas in which the two-peaked signature of first order replica symmetry breaking, predicted by Eq. (10), is in random lasers, wherein stimulated emission is complicated by the medium in one manner or another [30, 33, 99, 108]. Because the energy density is controlled by the pump power, the latter acts as the inverse temperature. Thus, as the pump power increases, the nonlinearity in the system plays the role of corrugating the energy landscape, analogous to the low temperature behavior in a glass. On the other hand, for low pump power, the cavity modes are ostensibly independent of each other, which is analogous to the paramagnetic phase of the spin glass. Importantly, a random laser has a large number of metastable states whereas a chaotic laser has a small number of modes that can exhibit exponential path divergence. This leads to different spectral properties for each type of laser.

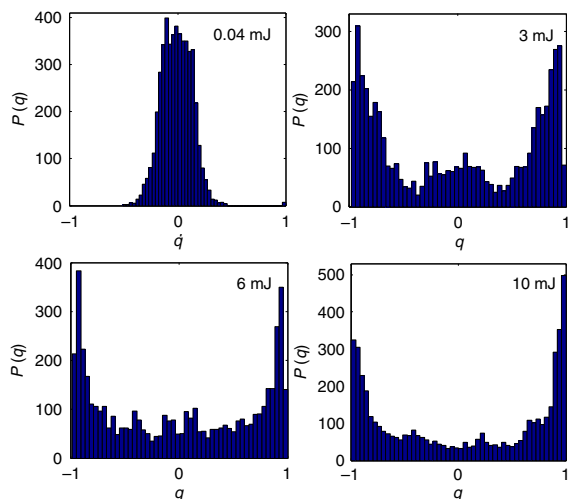


FIG. 7. The distribution  $P(q)$  of the overlap  $q_{\alpha\beta}$  for different pump energies (shown in the inset) from [30]. As discussed in the text, the pump energy plays the role of the inverse temperature. As the pump energy increases the distribution of first order replica symmetry breaking appears.

Ghofraniha *et al.* [30] quantify spectral data from a random laser and analyze the fluctuations in emission between different shots. The idea is that each emission spectrum defines a replica, say  $\alpha$ , of the random laser under the same conditions. If the intensity fluctuation func-

tion is  $\Delta_\alpha(k) = I_\alpha(k) - \bar{I}(k)$ , where  $\bar{I}(k) = \sum_\alpha I_\alpha(k)/N_s$  is the average intensity at each wavelength indexed by  $k$ , then the Parisi overlap function, Eq. (9), becomes

$$q_{\alpha\beta} = \frac{\sum_k \Delta_\alpha(k) \Delta_\beta(k)}{\sqrt{\sum_k \Delta_\alpha^2(k)} \sqrt{\sum_k \Delta_\beta^2(k)}}. \quad (11)$$

It is observed that there is a much larger spectral variation at strong pumping (“low T”) and the variance of the emission intensity changes discontinuously at a particular energy, exhibiting a phase transition (Fig. 3 of [30]). After having generated many shots a direct measurement of  $P(q)$  is realized and demonstrates first order replica symmetry breaking as shown in Fig. 7. That this same result is found in different random laser systems [99] speaks to the robust nature of this demonstration of replica symmetry breaking.

Whilst we have dwelled upon the realization of replica symmetry breaking, through the lens of fluctuations, stochasticity and disorder, Giorgio Parisi has been involved in uncovering the scaffolding of, and developing the tendrils between, a stunning range of physical systems. A subset of these include stochasticity in quantum field theory, the intermittency of turbulence, Euclidean random matrices, non-equilibrium fluctuations in glasses, stochastic interfacial motion, granular matter and the role of random fluctuations in controlling Earth’s climate states over long epochs.

## VI. SUMMARY

Clearly this year’s Laureates have made groundbreaking contributions to our understanding of complex physical systems in their broadest sense, from the microscopic to the global. They show that without a proper accounting of disorder, noise and variability, determinism is just an illusion. Indeed, the work recognized here reflects in part the comment ascribed to Richard Feynman (Nobel Laureate 1965), that he “Believed in the primacy of doubt, not as a blemish on our ability to know, but as the essence of knowing.”, [32].

Recognizing the work of this troika reflects the importance of understanding that no single prediction of anything can be taken as inviolable truth, and that without soberly probing the origins of variability we cannot understand the behavior of any system. Therefore, only after having considered these origins do we understand that global warming is real and attributable to our own activities, that a vast array of the phenomena we observe in nature emerge from an underlying disorder, and that embracing the noise and uncertainty is an essential step on the road towards predictability.

[1] Agarwal S, Wettlaufer, J S. 2018. Fluctuations in Arctic sea-ice extent: comparing observations and climate

models. *Phil. Trans. R. Soc. A* **376**, 20170332.

[2] Alley RB. 2000. Ice-core evidence of abrupt climate

- changes. *Proc. Nat. Acad. Sci. USA* **97**, 1331-1334.
- [3] Anderson PW. 1988. Spin Glass I: A Scaling Law Rescued. *Phys. Today* **41** 526.
- [4] Archer D. and Pierrehumbert RP. (Editors). 2011. *The Warming Papers: The Scientific Foundation for the Climate Change Forecast*. Wiley-Blackwell, Hoboken, NJ, 432 Pages.
- [5] Archer D. 2006. *Global Warming: Understanding the Forecast*, Wiley 208 pages
- [6] Arrhenius A. 1896. On the Influence of Carbonic Acid in the Air upon the Temperature of the Ground, *Phil. Mag.* **41**, 237-275.
- [7] Basak, S., Blanco, A., López, C. 2016. Large fluctuations at the lasing threshold of solid-and liquid-state dye lasers. *Sci. Rep.* **6**, 32134.
- [8] Batchelor GK. 1953. *The Theory of Homogeneous Turbulence*. Cambridge: Cambridge Univ. Press. 212 pg.
- [9] Behringer, RP. Chakraborty, B. 2019. The physics of jamming for granular materials: a Review. *Rep. Prog. Phys.* **82** 012601.
- [10] Benzi R, Paladin G, Parisi G, Vulpiani A. 1984. On the multifractal nature of fully developed turbulence and chaotic systems. *J. Phys. A* **17** 3521-31.
- [11] Berner J, and 26 others. 2017. Stochastic Parameterization: Toward a New View of Weather and Climate Models. *Bull. Am. Met. Soc.* **98**(3) 565-587.
- [12] Binder K, Young AP. 1986. Spin glasses: Experimental facts, theoretical concepts, and open questions. *Rev. Mod. Phys.* **58**, 801.
- [13] Blandin A. 1978. Theories versus experiments in the spin glass systems. *J. Phys. Coll.* **39 C6**, C6-1499-C6-1516.
- [14] Bray AJ, Moore MA. 1978. Replica symmetry breaking in spin-glass theories. *Phys. Rev. Lett.* **41**,1068.
- [15] Budyko MI. 1969. The effect of solar radiation variations on the climate of the Earth. *Tellus* **21**, 611-619.
- [16] Charbonneau, P. Corwin, EI. Parisi, G. Zamponi, F. 2012. Universal Microstructure and Mechanical Stability of Jammed Packings *Phys. Rev. Lett.* **109**, 205501.
- [17] Charbonneau, P. Kurchan, J. Parisi, G. Urbani, P. Zamponi, F. 2017. Glass and Jamming Transitions: From Exact Results to Finite Dimensional Descriptions. *Annu. Rev. Cond. Matt. Phys.* **8**, 265.
- [18] Charney JG, Fjörtoft R, von Neumann J. 1950. Numerical Integration of the Barotropic Vorticity Equation. *Tellus* **2** (4), 237-254.
- [19] Charney JG, Arakawa A, Baker DJ, Bolin B, Dickenson RE, Goody RM, Leith CE, Stommel HM, Wunsch CI. *Carbon Dioxide and Climate: A Scientific Assessment*.
- [20] Culina, J. Kravtsov, S. and Monahan, A.H. 2011. Stochastic Parameterization Schemes for Use in Realistic Climate Models, *J. Atmos. Sci.* **68**, 284.
- [21] de Almeida JRL, Thouless DJ. 1978. Stability of the Sherrington-Kirkpatrick solution of a spin glass model, *J. Phys. A* **11**, 983.
- [22] Doering CR. 2016: *Mathematical Foundations of Stochastic Processes*. 2015 Program of Study: Stochastic Processes in Atmospheric and Oceanic Dynamics, J. S. Wettlaufer and O. Bühler, Eds., *Woods Hole Oceanographic Institution* Tech. Rep. WHOI-2016-05, 140, doi:10.1575/1912/8601.
- [23] Doering CR. 2020. Turning up the heat in turbulent thermal convection. *Proc. Nat. Acad. Sci. U.S.A.* **117**, 9671-9673.
- [24] Edwards SF, Anderson PW. 1975. Theory of spin glasses. *J. Physics F: Metal Physics*, **5**, 965.
- [25] EPICA community members. 2004. Eight glacial cycles from an Antarctic ice core. *Nature*, **429** 623-628.
- [26] Frankignoul C, Hasselmann K. 1977. Stochastic climate models, Part II. Application to sea-surface temperature anomalies and thermocline variability. *Tellus* **29**, 289305.
- [27] Gardiner, C. *Stochastic Methods*. Springer, Berlin Heidelberg, Germany, 4<sup>th</sup> edition, 2009.
- [28] Ghil M. 1976. Climate Stability for a Sellers-Type Model. *J. Atmos. Sci.* **33**, 3-20.
- [29] Ghil M, Lucarini V. 2020. The Physics of Climate Variability and Climate Change. *Rev. Mod. Phys.* **92**, 035002.
- [30] Ghofraniha N, Viola I, Di Maria F, Barbarella G, Gigli G, Leuzzi L, Conti C. 2015. Experimental evidence of replica symmetry breaking in random lasers. *Nat. Commun.* **6**, 6058 (See also Corrigendum in regards to Fig. 4).
- [31] Glantz MH, Katz RW, Nicholls N. 1991 *Teleconnections linking worldwide climate anomalies*. Vol. 535. Cambridge: Cambridge University Press. 535 pg.
- [32] Gleick J. 1992. *Genius: The Life and Science of Richard Feynman*, pp. 489 (Open Road Integr. Media, New York.)
- [33] Gomes, A., Raposo, E., Moura, A. *et al.* 2016. Observation of Lévy distribution and replica symmetry breaking in random lasers from a single set of measurements. *Sci. Rep.* **6**, 27987.
- [34] González, I.R.R., Raposo, E.P., Macêdo, A.M.S. *et al.* 2018. Coexistence of turbulence-like and glassy behaviours in a photonic system. *Sci. Rep.* **8**, 17046.
- [35] Guckenheimer, J. and Holmes, P. *Nonlinear Oscillations, Dynamical Systems, and Bifurcations of Vector Fields*. Springer, New York, NY, 1983. 462 pg.
- [36] Halsey TC, Jensen MH, Kadanoff LP, Procaccia I, Shraiman BI. 1986. Fractal measures and their singularities: the characterization of strange sets. *Phys. Rev. A* **33**, 1141-51.
- [37] Hammond, AP. Corwin, EI. 2020. Experimental observation of the marginal glass phase in a colloidal glass. *Proc. Nat. Acad. Sci. USA* **117**, 5714-5718.
- [38] Hansen J, Russell G, Rind D, Stone P, Lacis A, Lebedeff S, Travis L. 1983. Efficient three-dimensional global models for climate studies: Models I and II. *Mon. Wea. Rev.* **111**, 609-662.
- [39] Hamilton K. 2020. At the dawn of global climate modeling: the strange case of the Leith atmosphere model. *Hist. Geo Space Sci.* **11**, 93103.
- [40] Hasselmann K. 1966. Feynman diagrams and interaction rules of wave-wave scattering processes. *Rev. Geophys.* **4**, 1-32.
- [41] Hasselmann K. 1967. Non-linear interactions treated by the methods of theoretical physics (with application to the generation of waves by wind). *Proc. R. Soc. A* **299**, 77-100.
- [42] Hasselmann K. 1976. Stochastic climate models part I. Theory. *Tellus* **28**(6), 473-485.
- [43] Hasselmann K. 1979. On the Signal-to-Noise Problem in Atmospheric Response Studies. In: *Meteorology of Tropical Oceans*. Ed. by D.B. Shaw. London: Roy Meteorol Soc., pp. 251 – 259.
- [44] Hasselmann K. 1993. Optimal Fingerprints for the De-

- tection of Time-Dependent Climate Change. *J. Climate* **6**, 1957-1971.
- [45] Hasselmann K. 1997. Multi-Pattern Fingerprint Method for Detection and Attribution of Climate Change. *Clim. Dyn.* **13**, 601-611.
- [46] Hegerl G, Hasselmann K, Cubasch U, Mitchell JFB, Roeckner E, Voss R, Waszkewitz J. 1997. Multi-fingerprint detection and attribution analysis of greenhouse gas, greenhouse gas-plus-aerosol and solar forced climate change. *Clim. Dyn.* **13**, 613-634.
- [47] Hegerl G, North GR. 1997. Comparison of Statistically Optimal Approaches to Detecting Anthropogenic Climate Change. *J. Clim* **10**, 1125.
- [48] Hegerl G, Zwiers F, Tebaldi C. 2011. Patterns of change: whose fingerprint is seen in global warming? *Environ. Res. Lett.* **6**, 044025.
- [49] Hegerl G, Zwiers F. 2011. Use of models in detection and attribution of climate change. *WIREs Clim. Change* **2** 570-91.
- [50] Hopfield JJ. 1982. Neural networks and physical systems with emergent collective computational properties. *Proc. Nat. Acad. Sci. USA* **79**, 2554-2558.
- [51] Iyer KP, Scheel JD, Schumacher J, Sreenivasan KR. 2020. Classical 1/3 scaling of convection holds up to  $Ra=10^{15}$ . *Proc. Nat. Acad. Sci. USA* **117**, 7594-7598.
- [52] Jung T, Miller MJ, Palmer TN, Towers P, Wedi N, Achuthavarier D, Marx L. 2012. High-resolution global climate simulations with the ECMWF model in Project Athena: Experimental design, model climate and seasonal forecast skill. *J. Climate* **25**, 3155-3172.
- [53] Kirkpatrick S, Gelatt CD, Vecchi MP. 1983. Optimization by Simulated Annealing. *Science* **220**, 671-680.
- [54] Kirschvink JL. 1992. Late Proterozoic low-latitude global glaciation: The snowball Earth, in *The Proterozoic Biosphere*, edited by J. W. Schopf and C. Klein, pp. 51-52, Cambridge Univ. Press, New York.
- [55] Knutti R, Sedlacek J. 2013. Robustness and uncertainties in the new CMIP5 climate model projections. *Nature Climate Change* **3**, 369-373
- [56] Lorenz, EN. 1963. Deterministic nonperiodic flow. *J. Atmos. Sci.* **20**, 130-41.
- [57] Lorenz, EN. 1992. The slow manifold-What is it? *J. Atmos. Sci.* **49**, 2449-2451.
- [58] Lyubovtseva YS, Gvishiani AD, Soloviev AA, Samokhina OO, Krasnoperov RI. 2020. Sixtieth anniversary of the International Geophysical Year (1957-2017) - contribution of the Soviet Union. *Hist. Geo Space Sci.* **11**, 157171.
- [59] Majda AJ, Timofeyev I, and Vanden-Eijnden E. 2001. A mathematical framework for stochastic climate models. *Commun. Pure Appl. Math.* **54**, 891-974.
- [60] Manabe, S, Möller, F. 1961. On the radiative equilibrium and heat balance of the atmosphere. *Mon. Wea. Rev.* **89**, 503-32.
- [61] Manabe, S, Strickler, RF. 1964. Thermal equilibrium of the atmosphere with a convective adjustment *J. Atmos. Sci.* **21**, 361-85.
- [62] Manabe, S, Wetherald, RT. 1967. Thermal equilibrium of the atmosphere with a given distribution of relative humidity. *J. Atmos. Sci.* **24**, 241-259.
- [63] Manabe, S, Wetherald, RT. 1975. The Effects of Doubling the CO<sub>2</sub> Concentration on the climate of a General Circulation Model. *J. Atmos. Sci.* **32**, 3-15.
- [64] Mandelbrot, BB. 1974. Intermittent turbulence in self-similar cascades: divergence of high moments and dimension of the carrier. *J. Fluid Mech.* **62**, 331-58.
- [65] Mann, ME, Steinman, BA, and Miller, SK. 2020. Absence of internal multidecadal and interdecadal oscillations in climate model simulations. *Nat Commun* **11**, 1-9.
- [66] Malkus, WVR. 2001. Borders of disorder. *Stud. Appl. Math.* **107**, 325-336.
- [67] Meneveau, C. Sreenivasan, KR. 1987. Simple multifractal cascade model for fully developed turbulence. *Phys. Rev. Lett.* **59**, 1424-27.
- [68] Mézard M, Parisi G, Virasoro M. 1987. *Spin glass theory and beyond: An Introduction to the Replica Method and Its Applications*. World Scientific, Singapore. 476 pg.
- [69] Mézard M, Parisi G, Sourlas N, Toulouse G, Virasoro M. 1984. Nature of the spin-glass phase. *Phys. Rev. Lett.* **52**, 1156.
- [70] Mézard, M. Parisi, G. and Zecchina, R. 2002. Analytic and Algorithmic Solution of Random Satisfiability Problems. *Science* **297**, 812.
- [71] Mitchell JM Jr. 1966. Stochastic models of air-sea interaction and climatic fluctuation. (Symp. on the Arctic Heat Budget and Atmospheric Circulation, Lake Arrowhead, Calif., 1966) Mem. RM-5233-NSF, The Rand Corp., Santa Monica.
- [72] Moon W, Agarwal S, Wettlaufer JS. 2018. Intrinsic Pink-Noise Multidecadal Global Climate Dynamics Mode. *Phys. Rev. Lett.* **121**, 108701.
- [73] Moon W, Wettlaufer JS. 2019. Coupling functions in climate. *Phil. Trans. R. Soc. A* **377**, 20190006.
- [74] Moura, A., et al. 2017. Replica Symmetry Breaking in the Photonic Ferromagneticlike Spontaneous Mode-Locking Phase of a Multimode Nd:YAG Laser, *Phys. Rev. Lett.* **119**, 163902.
- [75] Möller, F. 1963. On the influence of changes in the CO<sub>2</sub> concentration in air on the radiation balance of the Earth's surface and on the climate. *J. Geophys. Res.* **68**, 3877-86.
- [76] Munk WH. 1960. Smoothing and persistence. *J. Meteor.* **17**, 92-93.
- [77] Orszag SA. 1971. Galerkin approximations to flows within slabs, spheres, and cylinders. *Phys. Rev. Lett.* **26**, 1100-1103.
- [78] North GR. 1975. Theory of energy-balance climate models. *J. Atmos. Sci.* **32**, 2033-43.
- [79] North GR. 1975. Analytical solution to a simple climate model with diffusive heat transport. *J. Atmos. Sci.* **32** (11), 1301-07.
- [80] Palmer TN. 2001. A nonlinear dynamical perspective on model error: a proposal for nonlocal stochastic-dynamic parametrization in weather and climate prediction models. *Q.J.R. Meteorol. Soc.* **127**, 279-304.
- [81] Palmer TN. 2017. The primacy of doubt: Evolution of numerical weather prediction from determinism to probability. *J. Adv. Model. Earth Syst.* **9**(2), 730-734.
- [82] Parisi G. 1979. Toward a Mean Field Theory for Spin Glasses. *Phys. Lett. A* **73**, 203.
- [83] Parisi G. 1979. Infinite number of order parameters for spin-glasses *Phys. Rev. Lett.* **43**, 1754.
- [84] Parisi G. 1980. Magnetic properties of spin glasses in a new mean field theory. *J. Phys. A: Math. Gen.* **13**, 1887.
- [85] Parisi G. 1983. Order parameter for spin-glasses. *Phys. Rev. Lett.* **50**, 1946.

- [86] Parisi G. 1988. *Statistical Field Theory*. (Addison-Wesley, Redwood City, CA. pp. 352)
- [87] Parisi G. 2005. Brownian motion *Nature* **433**, 221.
- [88] Parisi G, Frisch U. 1985. On the singularity structure of fully developed turbulence. In *Turbulence and Predictability in Geophysical Fluid Dynamics*, ed. M Ghil, R Benzi, G Parisi, pp. 84-87. Amsterdam: North-Holland.
- [89] Parisi, G and Zamponi F. 2010. Mean-field theory of hard sphere glasses and jamming. *Rev. Mod. Phys.* **82** (1), 789.
- [90] Pierangeli, D., Tavani, A., Di Mei, F. *et al.* 2017. Observation of replica symmetry breaking in disordered nonlinear wave propagation. *Nat Commun* **8**, 1501.
- [91] Pierrehumbert RT. 2011. *Principles of Planetary Climate*. Cambridge Univ. Press, Cambridge, pp. 684.
- [92] Pomeau, Y. The long and winding road. 2016. *Nature Phys.* **12**, 198-199.
- [93] Rainone, C. Urbani, P. 2016. Following the evolution of glassy states under external perturbations: the full replica symmetry breaking solution. *J. Stat. Mech. Th. & Exp.* 053302.
- [94] Rawlins F, Ballard SP, Bovis KJ, Clayton AM, Li D, Inverarity GW, Payne TJ. 2007. The Met Office global four-dimensional variational data assimilation scheme. *Q. J. Royal Meteorol. Soc.* **133**, 347-362.
- [95] Rissone, P. Corwin, EI. Parisi, G. 2021. Long-Range Anomalous Decay of the Correlation in Jammed Packings. *Phys. Rev. Lett.* **127**, 038001.
- [96] Read N. 2014. Short-range Ising spin glasses: The metastate interpretation of replica symmetry breaking. *Phys. Rev. E* **90** 032142.
- [97] Saltzman B. 1962. Finite amplitude free convection as an initial value problem-I. *J. Atmos. Sci.* **19**, 329-341.
- [98] Santer, BD *et al.*, 2019. Celebrating the anniversary of three key events in climate change science. *Nature Clim. Change* **9**, 180182.
- [99] Sarkar, A., Shivakiran Bhaktha, B.N.; Andreassen, J. 2020. Replica Symmetry Breaking in a Weakly Scattering Optofluidic Random Laser. *Sci. Rep.* **10**, 2628.
- [100] Schrag DP, Berner RA, Hoffman PF, Halverson GP. 2002. On the initiation of a snowball Earth, *Geochem. Geophys. Geosyst.* **3**(6), doi:10.1029/2001GC00219.
- [101] Sellers WD. 1969. A Global Climatic Model Based on the Energy Balance of the Earth-Atmosphere System. *J. Appl. Meteor.* **8**, 392-400.
- [102] Sherrington, D. and Kirkpatrick, S. 1975. Solvable Model of a Spin-Glass. *Phys. Rev. Lett.* **35**, 1792.
- [103] Strogatz, S.H. *Nonlinear Dynamics and Chaos*. Westview Press, 2000. 512 pg.
- [104] Sreenivasan, KR. Antonia, RA. 1997. The phenomenology of small scale turbulence. *Annu. Rev. Fluid Mech.* **29**, 435-72.
- [105] Temam R. *Infinite-Dimensional Dynamical Systems in Mechanics and Physics*. Springer, New York, NY, 1997.
- [106] Thouless DJ, Anderson PW, Palmer RG. 1977. Solution of 'Solvable model of a spin glass'. *Phil. Mag. A* **35**, 593.
- [107] Thouless, DJ. 1988. *Phys. Today* **41** (12), 110.
- [108] Tommasi, F., Ignesti, E., Lepri, S., Cavalieri, S. 2016. Robustness of replica symmetry breaking phenomenology in random laser. *Sci. Rep.* **6**, 37113.
- [109] Tyndall J. 1861. On the absorption and radiation of heat by gases and vapours, and on the physical connexion of radiation, absorption, and conduction. *Philosophical Magazine Series 4* **22**, 169-194; 273-285.
- [110] Untersteiner N. 2009. International Geophysical Year, 1957-1958: Drifting Station Alpha Documentary Film, National Snow and Ice Data Center, doi.org/10.7265/N5MK69TW or nsidc.org/data/g02184.
- [111] Wettlaufer, JS. 2016. *Editorial*. Climate Science: An Invitation for Physicists. *Phys. Rev. Lett.* **116**, 150002.
- [112] Wiin-Nielsen A. 1991. The birth of numerical weather prediction. *Tellus A* **43** (4), 36-52.
- [113] Wunsch, C. *Modern Observational Physical Oceanography: Understanding the Global Ocean* (Princeton University Press, Princeton, NJ, 2015).
- [114] The founders of this field are all now deceased. In the 50's Stommel and Veronis began collaborating at the IAS within the von Neumann and Charney project, but their ultimate approach was to understand detailed processes rather than to study forecasting. A GFD school began in 1959: "with the aim of introducing a then relatively new topic in mathematical physics, geophysical fluid dynamics, to graduate students in physical sciences. It has been held each summer since and promotes an exchange of ideas among the many distinct fields that share a common interest in the nonlinear dynamics of rotating, stratified fluids. These fields include classical fluid dynamics, physical oceanography, meteorology, astrophysics, planetary atmospheres, geological fluid dynamics, hydromagnetics, and applied mathematics." (<https://gfd.who.edu>)
- [115] It is worth emphasizing that before the availability of computing, progress in explaining observations or making predictions in all of the physical sciences, including climate science, was made using pencil and paper calculations. Computers changed this completely and in an era precisely during which both theory and numerical modeling in this field were developing. For this reason, a conceptual bifurcation occurred in which "numerical realism" and "simple" theory began to evolve separately and the generality of the latter was largely viewed as a handicap rather than a great benefit, whereas numerical climate models are only specifically relevant to the system under study [111]. After roughly half a century the theory of climate is now demonstrating its realism as well as having touched many fields in dynamical systems along the way. This is due to the fact that nonlinear systems create emergent phenomena whereas GCMs act in a variety of ways as a filters of high frequency processes.